Mon. Not. R. Astron. Soc. **266**, 903–909 (1994)

First results from the UHRF: ultra-high-resolution observations of interstellar CH, CH^+ and CN towards ζ Ophiuchi

I. A. Crawford,[1,2] M. J. Barlow,[2] F. Diego[2] and J. Spyromilio[1]

[1] *Anglo-Australian Observatory, PO Box 296, Epping, NSW 2121, Australia*

[2] *Department of Physics and Astronomy, University College London, Gower Street, London WC1E 6BT*

Received 1993 September 13; in original form 1993 July 28

ABSTRACT

We present ultra-high-resolution observations ($R > 700\,000$) of interstellar CH, CH^+ and CN towards ζ Oph obtained with the newly commissioned Ultra-High-Resolution Facility (UHRF) at the AAT. The molecular lines have all been fully resolved, and we discuss their implications for this well-studied molecular sightline. The CH and CN lines each consist of two narrow ($b \approx 0.5$ km s^{-1}) components separated by 1.13 ± 0.10 km s^{-1}; an additional broad ($b = 1.8$ km s^{-1}) component is present in CH. We show that the very broad ($b = 2.1$ km s^{-1}) CH^+ line profile is consistent with the formation of this molecule in warm haloes surrounding the cold cores responsible for the narrow CH and CN components.

Key words: line: profiles – stars: individual: ζ Oph – ISM: molecules.

1 INTRODUCTION

The bright ($V = 2.6$) southern O9.5V star ζ Ophiuchi has one of the richest known interstellar sightlines (e.g. Herbig 1968; Morton 1975), and its study has come to provide the observational underpinning for a wide range of models describing the physical and chemical state of diffuse molecular clouds. Here we report observations of interstellar lines due to the molecules CH, CH^+ and CN towards ζ Oph, obtained with the new Ultra-High-Resolution Facility (UHRF) at the Anglo-Australian Telescope (AAT). This instrument, an echelle spectrograph capable of resolving powers of up to $R \approx 10^6$, was commissioned at the AAT in 1992 July (for details, see Barlow et al., in preparation; Diego et al., in preparation).

The present observations were obtained in 1993 May, and to our knowledge comprise the highest resolution optical spectra of interstellar molecules yet obtained. They complement, and largely confirm, the earlier very-high-resolution observations ($R = 600\,000$) of Lambert, Sheffer & Crane (1990), although our interpretation of the line profiles is somewhat different.

2 OBSERVATIONS AND DATA REDUCTION

Table 1 lists the lines observed, the adopted rest wavelengths and oscillator strengths (CH, CN: Black & van Dishoeck 1988; CH^+: Lambert & Danks 1986), the spectral resolution of each observation, exposure times, the total number of continuum counts (e^-) above background, and the measured equivalent widths. The detector was the AAO blue Thomson CCD (1024×1024 19-μm pixels), and the spectra were extracted from the CCD images using the FIGARO data reduction package (Shortridge 1988). The spectra are shown in Fig. 1. The observed line profiles are plotted as histograms, where each bin corresponds to a collapsed 19-μm-wide CCD column. Theoretical line profiles (discussed in Section 3) are plotted as smooth curves superimposed on the observed profiles.

Three aspects of the data calibration procedure deserve special comment.

2.1 Wavelength calibration

Wavelength calibration was performed by means of a Th–Ar lamp. In both the CH and CN spectral regions, four Th–Ar lines were identified within the ≈ 2-Å spectral coverage of the detector. Over this small spectral range the dispersion is almost linear, and a straight-line fit to the four Th–Ar lines in both regions resulted in negligible rms residuals (of the order of 10^{-4} Å, or 0.01 km s^{-1}).

The CH^+ spectral region was found to contain only one identified Th–Ar line, with several weaker (unidentified) lines present in the same spectral region. The wavelengths of the latter were obtained by fitting a second-order polynomial to five known Th–Ar lines which were found to occur within an interval of 6.5 Å, bracketing the CH^+ wavelength. The rms residual to this fit was 0.001 Å, which may therefore be

taken as a guide to the accuracy of the wavelengths of the (previously unmeasured) Th–Ar lines within 2 Å of the CH^+ wavelength. Thus, although the wavelength calibration of this region is somewhat more uncertain than that for the other molecules, the velocity scale should still be better than 0.07 km s^{-1}.

2.2 Resolution

The Th–Ar comparison lines are easily resolved by the UHRF, so the instrumental resolution was determined with the aid of a stabilized He–Ne laser. This yielded $R \equiv \lambda/\Delta\lambda = 940\,000$ (0.32 km s^{-1} FWHM) at the wavelength of the laser line (6328.160 Å). From a consideration of the optical design of the spectrograph (Diego et al., in preparation), we expect this resolution to hold for all wavelengths.

This assumption was checked by deconvolving the laser profile from the profiles of thorium lines found in the same spectral region, thereby obtaining the *intrinsic* widths of the latter (0.43 ± 0.01 km s^{-1}). This then enabled us to determine the instrumental resolution at each of the interstellar line wavelengths from the observed widths of nearby thorium lines. For reasons still being investigated, this indirect analysis yielded the somewhat lower resolving powers of 700 000 (CN) and 800 000 (CH, CH^+). However, in all cases the instrumental profile is narrower than the observed interstellar lines, even for these lower resolving powers. The interstellar lines have therefore been fully resolved, and it can be shown that, even for the narrowest of them (CN), an uncertain resolving power in the range 700 000 to 940 000 makes no significant difference to the line profile parameters derived in Section 3.

2.3 Background correction

The spectra were obtained by means of a new 35-slice confocal image slicer (Diego 1993), which takes light from the central 1.5 arcsec of the stellar seeing disc and converts it into a slit of width ≈ 30 μm. The resulting very long (20-mm) slit is compressed by a cylindrical lens to ≈ 1 mm on the detector. This arrangement has greatly increased the throughput of the instrument (Diego et al., in preparation), but makes it impossible to measure the scattered light background directly from the interorder region. Moreover, in the blue, where the orders are very close together, there is a danger of part of an adjacent order clipping the edge of the cylindrical lens, and being focused on to the detector along with the order to be observed.

There is evidence that the UHRF is currently affected by background light to a significant degree (Barlow et al., in preparation), and steps are presently underway to quantify and reduce this. For the time being, we estimate the background correction by comparing our equivalent widths (Table 1) with accurate measurements by other authors. In the case of CH, Danks, Federman & Lambert (1984) obtained an equivalent width of 17.8 ± 0.9 mÅ, which would imply that our value (15.8 mÅ) has been diluted by a background amounting to 11 per cent of the continuum intensity. For CH^+, most recent measurements agree on an equivalent width within 0.5 mÅ of 23.5 mÅ (Vanden Bout & Snell 1980; Lambert & Danks 1986; Hawkins, Craig & Meyer 1993), which implies that our uncorrected background amounts to (7 ± 2) per cent. For the CN $R(0)$ line, our value (7.6 mÅ) is essentially identical to the values obtained by Federman, Danks & Lambert (1984) and Crane et al. (1986), but somewhat smaller than the value of 8.16 mÅ obtained by Hawkins et al. (1993). As we are convinced that the present observations are afflicted by background light at least to some extent, and as this must cause the equivalent widths to be underestimated, we here adopt the value of Hawkins et al. (which implies a background correction of 7.3 per cent), and suggest that the measurements of Federman et al. (1984) and Crane et al. (1986) may themselves not have been fully corrected for scattered light.

On the basis of these comparisons, we estimate that scattered light amounting to approximately (8 ± 4) per cent of the continuum intensity is present in the spectra discussed here. This background was subtracted prior to normalization of the spectra, as shown in Fig. 1, and has been allowed for in the following analysis. We note that, while this uncertainty in the background has had a small effect ($\lesssim \pm 7$ per cent) on the derived column densities, it has had a negligible effect on the measured linewidths which are our principal concern here.

3 INDIVIDUAL MOLECULAR LINE PROFILES

A line profile analysis was performed using the DIPSO spectrum analysis program (Howarth & Murray 1988). The results are given in Table 2; we briefly discuss the results obtained for the individual lines below.

3.1 CH

The CH $R_2(1)$ line is split owing to Λ-doubling in the $^2\Pi$ ground state of the molecule, the two components being separated by 1.43 km s^{-1} (Black & van Dishoeck 1988). However, as the two Λ-doublet components have equal strength, the observed asymmetry (Fig. 1a) immediately indicates the presence of additional, unresolved, velocity structure. Indeed, Liszt (1979) found two velocity components, separated by approximately 1.2 km s^{-1}, in his 9-cm ($F = 1$–1) CH emission spectrum towards this star. Also, Black & van Dishoeck (1988) predicted an asymmetric CH absorption-line profile, very similar to that observed (cf. their fig. 3), on the basis of the velocity structure found in the CO $J = 1$–0 emission line by Langer, Glassgold & Wilson (1987).

A high-spatial-resolution (12-arcsec) study of CO $J = 1$–0 and 2–1 emission towards ζ Oph by Le Bourlot, Gérin & Pérault (1989) found two velocity components separated by 1.18 km s^{-1}. Line profile modelling has indicated that two components with this separation can accurately account for the structure within the core of the CH line, although an additional, broader component is required to fit the wings of the profile. Thus at least three discrete velocity components are required to fit the observed CH line profile (Table 2), as demonstrated earlier by Lambert et al. (1990). We find the wings of the CH profile to be less extensive than found by Lambert et al., and the velocity dispersion of the broad component is significantly narrower in our case ($b = 1.8 \pm 0.5$ km s^{-1}, as opposed to the 3.1 ± 0.2 km s^{-1} of Lambert et al.). We further note that in our model the velocity of the broad component is (to within the errors) the same as that of the strongest narrow component.

3.2 CH^+

Lambert et al. (1990) found that they could fit the CH^+ $R(0)$ line with a single Gaussian. We agree that a single component gives a good fit (dotted curve in Fig. 1b), but find that it is less than perfect in the blue wing of the profile. Moreover, as the CH and CN lines have, respectively, three and two velocity components (and the CO line is also known to be double; Le Bourlot et al. 1989), there is reason to suspect that the broad CH^+ line may in reality be an unresolved blend. Theoretical line profiles were therefore constructed in order to determine whether the overall profile is consistent with the assumption that the multiple velocity structure found for CH and CN is also present in CH^+.

Initially, a two-component model was attempted, with two CH^+ components having the same velocity separation as the narrow CH components. This gave a good fit to the core of the line, but produced a poorer fit in the wings than the assumption of a single component. Our best fit (solid line in Fig. 1) involves three components. Two of these are relatively narrow (with essentially the same velocity separation as the CN components and the two narrow CH components); the third is broader, and may be physically associated with the broad CH component. If this interpretation is accepted, we see that the CH^+ components are significantly broader than their CH counterparts (Table 2). Finally, we note that on the basis of very high S/N ratio observations Crane, Hegyi & Lambert (1991) have reported the presence of a very broad ($b = 9.9$ km s^{-1}), shallow (central depth ~1 per cent), CH^+ component. We found no evidence for this component in our data, although it is doubtful whether we would expect to see it, given its extreme weakness and our S/N ratio (we note that it seems not to have been detected by Lambert et al. 1990 either).

3.3 CN

Both the $R(0)$ and $R(1)$ lines of the CN $B^2\Sigma^+$–$X^2\Sigma^+$ system were observed; the $P(1)$ line (3875.764 Å) cannot be obtained in the same frame as the other two lines, and was not observed. The line referred to as $R(0)$ for convenience is, in fact, a blend of the $R_1(0)$ and $^RQ_{21}(0)$ lines, which are separated by 0.27 km s^{-1} and have oscillator strengths in the ratio 2:1 (e.g. Federman et al. 1984). Similarly, the $R(1)$ line is a blend of the $R_1(1)$, $R_2(1)$ and $^RQ_{21}(1)$ lines (with an overall separation of 0.45 km s^{-1}). As this structure is on a scale comparable to our resolution, it has been included in the line profile analysis.

We find two narrow CN velocity components with velocity separations essentially the same as found by Le Bourlot et al. (1989) for the CO lines. We confirm the result of Lambert et al. (1990) that there is no evidence for a broad CN component corresponding to that found for CH.

4 DISCUSSION

4.1 Linewidths and cloud temperatures

One of the most important applications of the UHRF arises from its ability to resolve interstellar absorption-line profiles fully, thereby revealing the thermal and kinematic information that these profiles contain. All four molecular lines discussed here have been fully resolved (i.e. are found to be significantly broader than the instrumental resolution), with the result that the intrinsic velocity dispersions (b values) have been accurately determined (Table 2). The velocity dispersion is related to the kinetic temperature, T_k, and the rms turbulent velocity along the line of sight, v_t, through the expression

$$b = \left(\frac{2kT_k}{m} + 2v_t^2 \right)^{1/2}, \qquad (1)$$

where k is Boltzmann's constant and m is the mass of the species observed. The b values may therefore be used to obtain upper limits to the kinetic temperature by assuming turbulent motions to be absent. Alternatively, as the actual kinetic temperature of the molecular gas towards ζ Oph is reasonably well constrained at $T_k = 30 \pm 10$ K from the observed rotational excitation of C_2 (albeit under the assumption of a single velocity component; van Dishoeck & Black 1986), the observed b values may be used to estimate v_t. These values are given in Table 3. It will be seen that (with the exception of CH^+ and the broad CH component) the

Table 1. Interstellar molecular lines observed towards ζ Oph with the UHRF. Δv is the instrumental resolution (FWHM; Section 2.2), and w_λ gives the measured equivalent widths (2σ statistical errors); there is evidence that these values underestimate the true equivalent widths by (8 ± 4) per cent owing to uncorrected scattered light (Section 2.3). The CH observations were obtained through thin cloud, hence the longer exposure time for the same number of counts.

Mol.	Line	λ (Å)	f	Δv (FWHM) (km s^{-1})	Total Exp. (n x exp)	Counts (e^-)	w_λ (mÅ)
CH	$R_2(1)$	4300.313	5.06×10^{-3}	0.37 ± 0.02	3 × 600s	2.3×10^4	15.8 ± 0.2
CH^+	$R(0)$	4232.548	5.50×10^{-3}	0.39 ± 0.02	2 × 600s	2.3×10^4	21.9 ± 0.3
CN	$R(0)$	3874.607	3.38×10^{-2}	0.42 ± 0.02	1 × 1800s	3.0×10^4	7.6 ± 0.1
CN	$R(1)$	3873.999	2.25×10^{-2}	0.42 ± 0.02	1 × 1800s	3.0×10^4	2.3 ± 0.1

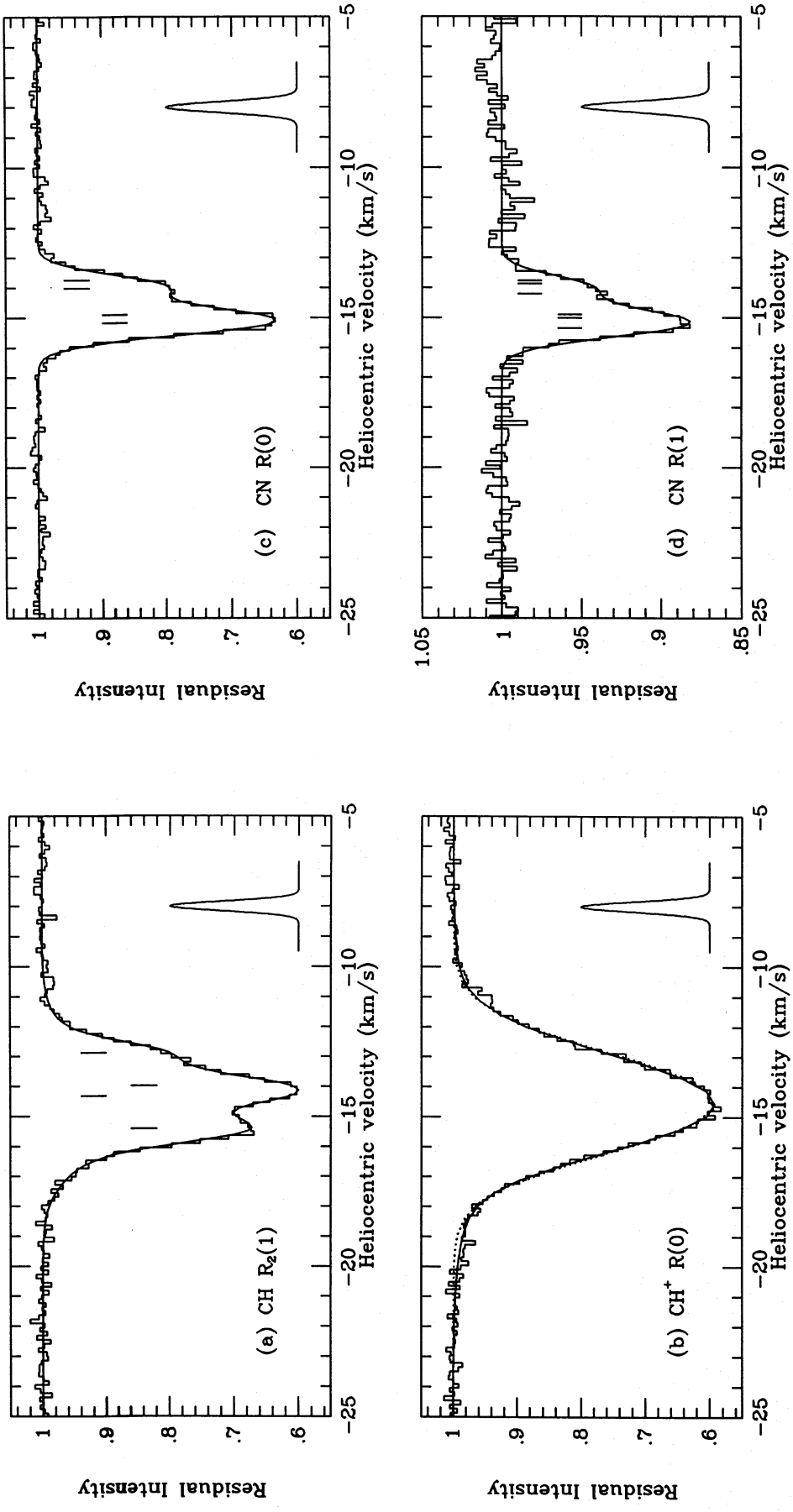

Figure 1. Profiles of the interstellar absorption lines due to CH, CH^+ and CN observed towards ζ Oph with the UHRF. The observed data are plotted as histograms; the smooth curves are theoretical profiles with the parameters given in Table 2. Insets indicate the instrumental resolution (Table 1). Vertical tick marks indicate the locations of the Λ-doublet components in CH (drawn for the two narrow components only), and the unresolved rotational structure within the CN $R(0)$ and $R(1)$ lines. In the case of CH^+, the dotted line shows the best fit obtained under the assumption of a single velocity component (see text).

upper limits to the temperature implied by the b values are of the order of a few hundred K, and that these correspond to turbulent velocities of around 0.3 km s^{-1} if a kinetic temperature of 30 K is assumed. Clearly, if the temperature is higher (closer to the 60 K favoured by Danks & Lambert 1983), the corresponding turbulent velocities will be lower. Thus this analysis implies subsonic turbulence, as the sound speed for 30-K interstellar gas is 0.44 km s^{-1} (rising to 0.62 km s^{-1} at 60 K). Lambert et al. (1990) obtained similar values for the temperature and turbulence of these components, although their slightly higher values of v_t (0.6 ± 0.1 and 0.5 ± 0.2 km s^{-1}) are more consistent with (marginally) supersonic turbulence.

In the case of CH^+, and the broad CH component, the inferred maximum temperatures are much higher, of the order of several thousand degrees. Temperatures of this order are required to drive the endothermic reaction

$$C^+ + H_2 + 0.4\ \text{eV} \longrightarrow CH^+ + H,$$

so the present observations are consistent with the formation of CH^+ by this reaction in a hot molecular gas. Although interstellar shocks have long been advocated as a means of raising diffuse cloud temperatures to $T_k \gtrsim 2000$ K (e.g. Elitzur & Watson 1978; Draine 1986; Pineau des Forêts et al. 1986), this is not the only mechanism capable of producing temperatures of this order (e.g. Duley et al. 1992), and the tide of opinion is in fact turning away from the shock models, owing to their apparent inability to meet other observational constraints. These problems have been summarized recently by van Dishoeck (1992). Briefly, they arise because of the absence of the predicted velocity difference between CH and CH^+ (Crawford 1989; Lambert et al. 1990; Hawkins & Craig 1991; also this work, Section 4.2 below); the trend of increasing CH^+ column density with A_V (Gredel, van Dishoeck & Black 1992); the absence of CH^+ in molecular gas known to be subject to shocks (e.g. Cardelli et al. 1990); and the inability of the shock models to account for both CH^+ and the observed degree of H_2 rotational excitation (e.g. Hartquist, Flower & Pineau des Forêts 1990).

Of the alternative mechanisms that have been proposed, the possibility that CH^+ is formed in the warm interfaces between molecular clouds and a hot intercloud medium (Duley et al. 1992) is particularly attractive in the present context. As we have demonstrated (Section 3.2) that the overall CH^+ profile is consistent with each of the two narrow CH and CN components being physically associated with a (broader) CH^+ component, it seems plausible that the CH and CN components arise in two separate diffuse molecular clouds, both of which are surrounded by a warm, CH^+-producing envelope. Wide-angle (2 deg-square) mapping of CO emission has, in fact, suggested that the main molecular 'component' towards ζ Oph is actually formed by the overlapping edges of two foreground clouds (Barrett, Solomon & Mooney 1989), and our interpretation is consistent with this picture. Still to be explained is the broad CH component, and its associated CH^+, although the velocity coincidence

Table 2. Line profile parameters for the CH, CH^+, and CN lines observed towards ζ Oph with the UHRF. In addition to the quoted errors, column densities are subject to a further (systematic) error of $\lesssim 7$ per cent due to the uncertain background correction discussed in the text; velocities and b values are unaffected.

CH $R_2(1)$			CH+ $R(0)$*		
v_{helio} (km s^{-1})	b (km s^{-1})	Log N (cm^{-2})	v_{helio} (km s^{-1})	b (km s^{-1})	Log N (cm^{-2})
-14.70 ± 0.05	$0.58^{+0.05}_{-0.13}$	$13.00^{+0.12}_{-0.30}$	-15.08 ± 0.10	$1.70^{+0.30}_{-0.30}$	$13.14^{+0.08}_{-0.09}$
-14.60 ± 0.20	$1.80^{+0.50}_{-0.50}$	$12.99^{+0.11}_{-0.19}$	-14.98 ± 0.20	$3.70^{+0.30}_{-1.70}$	$12.65^{+0.20}_{-0.10}$
-13.60 ± 0.05	$0.50^{+0.50}_{-0.20}$	$12.65^{+0.10}_{-0.15}$	-13.88 ± 0.10	$1.80^{+0.20}_{-0.20}$	$13.13^{+0.07}_{-0.08}$
CN $R(0)$			CN $R(1)$		
v_{helio} (km s^{-1})	b (km s^{-1})	Log N (cm^{-2})	v_{helio} (km s^{-1})	b (km s^{-1})	Log N (cm^{-2})
-15.08 ± 0.05	$0.55^{+0.05}_{-0.10}$	$12.17^{+0.03}_{-0.07}$	-15.16 ± 0.05	$0.55^{+0.05}_{-0.10}$	$11.80^{+0.03}_{-0.07}$
....	....	....	....	....	....
-13.92 ± 0.05	$0.45^{+0.10}_{-0.10}$	$11.77^{+0.11}_{-0.07}$	-14.02 ± 0.05	$0.45^{+0.05}_{-0.10}$	$11.39^{+0.08}_{-0.09}$

*If the CH^+ line is fitted by a single component (dotted line in Fig. 1b) we have: $v_{helio} = -14.52 \pm 0.02$ km s^{-1}; $b = 2.1^{+0.1}_{-0.2}$ km s^{-1} (identical to the value found by Lambert et al. 1990); $\log N = 13.50^{+0.02}_{-0.02}$.

Table 3. Kinetic temperature upper limits, T_k^{ul}, for the molecular gas observed towards ζ Oph under the assumption of zero turbulence. If T_k is set to 30 K, the corresponding turbulent velocities, v_t, are given for the narrow CH and CN components; this information is omitted in the case of CH^+, and the broad CH component, for which T_k is clearly $\gg 30$ K.

CH

v_{helio} (km s^{-1})	b (km s^{-1})	T_k^{ul} (K)	v_t (km s^{-1})
−14.70	$0.58^{+0.05}_{-0.13}$	260^{+50}_{-110}	$0.39^{+0.04}_{-0.10}$
−14.60	$1.80^{+0.50}_{-0.50}$	2600^{+1600}_{-1200}	....
−13.60	$0.50^{+0.50}_{-0.20}$	200^{+590}_{-130}	$0.33^{+0.37}_{-0.16}$

CN

v_{helio} (km s^{-1})	b (km s^{-1})	T_k^{ul} (K)	v_t (km s^{-1})
−15.08	$0.55^{+0.05}_{-0.10}$	480^{+90}_{-160}	$0.38^{+0.04}_{-0.07}$
....	....	....	....
−13.92	$0.45^{+0.05}_{-0.10}$	320^{+70}_{-130}	$0.30^{+0.04}_{-0.08}$

CH^+

v_{helio} (km s^{-1})	b (km s^{-1})	T_k^{ul} (K)
−15.08	$1.70^{+0.30}_{-0.30}$	2300^{+870}_{-730}
−14.98	$3.70^{+0.30}_{-1.70}$	11000^{+2000}_{-8000}
−13.88	$1.80^{+0.20}_{-0.20}$	2500^{+600}_{-500}

suggests that this arises in warm gas associated with the stronger of the two narrow components, possibly as an outer halo surrounding the molecular cloud core (or, conceivably, as a common envelope to both molecular clouds). In this context we note that, on the basis of their recent *HST* observations, Federman et al. (1993) have suggested that the two main molecular components form clumps within a more extensive distribution of lower density (mainly atomic) gas.

4.2 Velocity structure

Our analysis finds no evidence for a velocity difference between the lines of CN and CH^+. In particular, if we assume that the broad CH^+ profile results from each of the CH and CN components being physically associated with a CH^+ component (Section 3.2), we find $v(CH^+) - v(CN) = 0.00 \pm 0.11$ and 0.04 ± 0.11 km s^{-1} for the two components identified in CN [Table 2, taking the CN velocities from the $R(0)$ line]. On the other hand, we find small, and formally significant, velocity differences between CH and CH^+ (and CN), with the CH velocity being between 0.3 and 0.4 km s^{-1} more positive. Such a shift is consistent with the results of Lambert et al. (1990, their table 2), which gave $v(CH) - v(CH^+) = 0.5 \pm 0.3$ km s^{-1}, and is in the same sense as the smaller shift of 0.23 ± 0.08 km s^{-1} determined by Hawkins & Craig (1991). It is possible that this shift represents actual velocity structure within the absorbing clouds, and additional observations are desirable in order to confirm this.

In any case, as already noted by Lambert et al. (1990) and Hawkins & Craig (1991), the absence of large velocity differences between these molecules, and especially the apparent identity of the CH^+ and CN velocities found here, is contrary to the predictions of the MHD shock models for CH^+ production.

4.3 The CN excitation temperature

The observation of both the CN $R(0)$ and $R(1)$ lines enables us to calculate the excitation temperature of this molecule from the observed column densities in the $N=0$ and $N=1$ rotational levels. Before performing this calculation, we note that the column density errors listed in Table 2 mostly arise from the uncertainties in the b values; as both $R(0)$ and $R(1)$ must, in reality, have identical b values, the errors on the ratios $N(N=1)/N(N=0)$ are actually less than implied by a straightforward propagation of the tabulated errors. If b is held constant, the column density errors arising from the fitting uncertainties were found to amount to approximately 0.02 dex (5 per cent) for all four CN lines. As noted in Section 2.2, there is an additional zero-level uncertainty, amounting to $\approx \pm 4$ per cent of the continuum intensity. However, although this has a small effect on the individual column densities ($\lesssim 4.5$ per cent in the case of the CN lines), its systematic nature ensures that it has a negligible ($\ll 1$ per cent) effect on the $(N=1)/(N=0)$ column density ratio.

Allowing for these various uncertainties, we obtain the following CN rotational excitation temperatures:

Component 1: $T_{01} = 2.79 \pm 0.10$ K,

Component 2: $T_{01} = 2.76 \pm 0.10$ K.

Both of these are consistent with the *COBE* result for the temperature of the microwave background ($T_{CMB} = 2.74 \pm 0.06$ K, Mather et al. 1990). Thus there is no evidence for additional electron-impact excitation of CN in either of these clouds. This result is consistent with relatively low molecular hydrogen densities (several hundred cm^{-3}) for the molecular cores of both clouds (as densities greater than about 10^3 cm^{-3} would be expected to produce a significantly higher excitation temperature; Black & van Dishoeck 1991).

5 CONCLUSION

We have presented ultra-high-resolution observations of CH, CH^+ and CN towards ζ Oph, these being the first scientific results from the new UHRF instrument at the AAT. A few aspects of the instrument remain to be fully characterized. Foremost among these is determination of the resolution at wavelengths other than that of the stabilized He-Ne laser (although the resolving power is in all cases constrained to lie in the range 700 000 to 940 000; Section 2.2), and the degree to which scattered light affects the observations (here estimated to be (8 ± 4) per cent of the on-order continuum intensity; Section 2.3). However, these uncertainties have not affected the primary aim of the present work, namely measurement of the intrinsic widths of the molecular lines towards this much-studied star.

Our results largely confirm those of Lambert et al. (1990), with both the CH and CN lines being found to consist of two narrow ($b \approx 0.5$ km s^{-1}) components separated by 1.13 ± 0.10 km s^{-1}. An additional broad ($b = 1.8 \pm 0.5$ km s^{-1}) component is also present in CH. We have shown that the broad ($b = 2.1$ km s^{-1}) CH^+ line profile is consistent with the presence of this molecule in warm haloes surrounding the cold cores responsible for the narrow CH and CN components. We have measured the CN rotational excitation temperature, and shown that this is consistent with equilibrium with the cosmic microwave background for both of the CN velocity components.

ACKNOWLEDGMENTS

We thank the Director and staff of the Anglo-Australian Observatory for their support and encouragement of the UHRF project, and PATT for the award of telescope time. We thank Dr Stuart Lumsden and the referee for critical readings of the manuscript. We are grateful to Dr I. D. Howarth for discussions, and for making some useful modifications to the DIPSO program. IAC is grateful to the Royal Society for the award of an Exchange Fellowship at the Anglo-Australian Observatory.

REFERENCES

Barrett J. W., Solomon P. M., Mooney T. J., 1989, BAAS, 21, 761
Black J. H., van Dishoeck E. F., 1988, ApJ, 331, 986
Black J. H., van Dishoeck E. F., 1991, ApJ, 369, L9
Cardelli J. A., Suntzeff N. B., Edgar R. J., Savage B. D., 1990, ApJ, 362, 551
Crane P., Hegyi D. J., Mandolesi N., Danks A. C., 1986, ApJ, 309, 822
Crane P., Hegyi D. J., Lambert D. L., 1991, ApJ, 378, 181
Crawford I. A., 1989, MNRAS, 241, 575
Danks A. C., Lambert D. L., 1983, A&A, 124, 188
Danks A. C., Federman S. R., Lambert D. L., 1984, A&A, 130, 62
Diego F., 1993, Appl. Opt., 32, 6284
Draine B. T., 1986, ApJ, 310, 408
Duley W. W., Hartquist T. W., Sternberg A., Wagenblast R., Williams D. A., 1992, MNRAS, 255, 463
Elitzur M., Watson W. D., 1978, ApJ, 222, L141
Federman S. R., Danks A. C., Lambert D. L., 1984, ApJ, 287, 219
Federman S. R., Sheffer Y., Lambert D. L., Gilliland R. L., 1993, ApJ, 413, L51
Gredel R., van Dishoeck E. F., Black J. H., 1992, in Singh P. D., ed., Proc. IAU Symp. 150, Astrochemistry of Cosmic Phenomena. Kluwer, Dordrecht, p. 153
Hartquist T. W., Flower D. R., Pineau des Forêts G., 1990, in Hartquist T. W., ed., Molecular Astrophysics – A Volume Honouring Alexander Dalgarno. Cambridge Univ. Press, Cambridge, p. 99
Hawkins I., Craig N., 1991, ApJ, 375, 642
Hawkins I., Craig N., Meyer D. M., 1993, ApJ, 407, 185
Herbig G. H., 1968, Z. Astrophys., 68, 243
Howarth I. D., Murray J., 1988, Starlink User Note No. 50, Rutherford Appleton Laboratory
Lambert D. L., Danks A. C., 1986, ApJ, 303, 401
Lambert D. L., Sheffer Y., Crane P., 1990, ApJ, 359, L19
Langer W. D., Glassgold A. E., Wilson R. W., 1987, ApJ, 322, 450
Le Bourlot J., Gérin M., Pérault M., 1989, A&A, 219, 279
Liszt H. S., 1979, ApJ, 233, L147
Mather J. C. et al., 1990, ApJ, 354, L37
Morton D. C., 1975, ApJ, 197, 85
Pineau des Forêts G., Flower D. R., Hartquist T. W., Dalgarno A., 1986, MNRAS, 220, 801
Shortridge K., 1988, Starlink User Note No. 86, Rutherford Appleton Laboratory
Vanden Bout P. A., Snell R. L., 1980, ApJ, 236, 460
van Dishoeck E. F., 1992, in Singh P. D., ed., Proc. IAU Symp. 150, Astrochemistry of Cosmic Phenomena. Kluwer, Dordrecht, p. 143
van Dishoeck E. F., Black J. H., 1986, ApJ, 307, 332